

# Towards a molecular-level understanding of the reactivity differences for radical anions of juglone and plumbagin: an electrochemical and spectroelectrochemical approach

Lindsay S. Hernández-Muñoz,<sup>a</sup> Martín Gómez,<sup>b</sup> Felipe J. González,<sup>a</sup> Ignacio González<sup>c</sup> and Carlos Frontana<sup>\*†a</sup>

Received 17th December 2008, Accepted 13th February 2009

First published as an Advance Article on the web 19th March 2009

DOI: 10.1039/b822684a

An electrochemical and spectroelectrochemical strategy is presented for evaluating reactivity differences in the semiquinone anions from naturally occurring quinones juglone (5-hydroxy-1,4-naphthoquinone) and plumbagin (2-methyl-5-hydroxy-1,4-naphthoquinone). By employing cyclic voltammetry and *in situ* spectroelectrochemical electron spin resonance measurements, it was found that while semiquinone species generated from plumbagin are stable radical anions in DMSO solution, the species generated from juglone are more reactive. These latter species are involved in a self-protonation process involving a slow rate of protonation ( $1.8\text{--}2.1\text{ mol L}^{-1}$ ) due to the mild acidity of the OH group at the C-5 position. This result is important when considering observed differences in biochemical reactivity for these quinones, particularly in cases where mediated cytotoxic action is provoked by these agents, as is discussed in this work.

## Introduction

Quinone compounds are widely distributed chemical groups in nature which play several different roles in living organisms.<sup>1–6</sup> In pharmaceutical terms, the use of quinones is widespread since they can act as therapeutic agents (*e.g.* anthracycline<sup>7–9</sup> and daunorubicin<sup>10–13</sup>) through several mechanisms including redox cycling, arylation, DNA intercalation, break induction of DNA strands, generation of free radicals and alkylation *via* quinone methide formation.<sup>6–13</sup>

It has been proposed that 1,4-naphthoquinone (**1**, Fig. 1) derivatives bearing at least one phenolic hydroxyl group are potent inhibitors of Topoisomerase type enzymes and they are used clinically in the therapy of solid cancers.<sup>3,14–16</sup> In other studies,<sup>17–21</sup> it has been demonstrated that the presence of hydroxy substituents on 1,4-naphthoquinones modulates the toxicity to cultured rat hepatocytes, decreasing in the series 5,8-dihydroxy-1,4-naphthoquinone (naptazarin **5**, Fig. 1), 5-hydroxy-1,4-naphthoquinone (juglone **2**), 1,4-naphthoquinone, 2-hydroxy-1,4-naphthoquinone (lawsone, **3**, Fig. 1).<sup>19,20</sup> These authors concluded that toxicity is due to free radical formation but is also related to an electrophilic addition component. Also, a study on structure-activity relationships revealed that the hydroxyl group

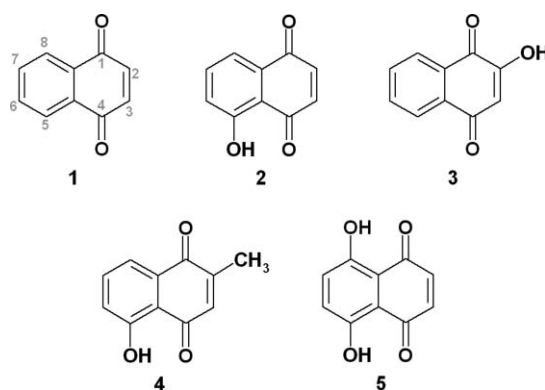


Fig. 1 Structures of different naphthoquinones. **1**: 1,4-naphthoquinone (NQ); **2**: juglone; **3**: lawsone; **4**: plumbagin; **5**: naptazarin.

of 5-hydroxy-1,4-naphthoquinone provokes a selective growth inhibition against the bacterium *C. perfringens*.<sup>21</sup>

In the case of quinones producing oxidative stress, the initiation of cell damage lies in the ability to form free-radical metabolites. The stability of these radical intermediates (formed through NADPH/NADP<sup>+</sup> cycling), seems to determine both the type and degree of biological activity. Unfortunately, evaluation of the stability of such intermediates is generally described by thermodynamic parameters, such as the standard reduction potential of the quinone on aqueous solutions,<sup>22,23</sup> where the radical is not stable and consequently, the potential data are influenced by homogenous chemical reactions. It has been also shown that differences in cytotoxic effects can occur upon changes in the concentration of the quinone; the toxic effect of plumbagin always increases upon greater concentrations, while for juglone, at certain values, cytotoxicity is hampered and remains constant.<sup>24</sup> Therefore, it would be useful to evaluate the evolution in chemical behavior during experiments at different concentrations of each

<sup>a</sup>Departamento de Química, Centro de Investigación y de Estudios Avanzados, Av. Instituto Politécnico Nacional No. 2508. Col. San Pedro Zacatenco, C. P. 07360, Mexico, DF, México

<sup>b</sup>Departamento de Sistemas Biológicos, Universidad Autónoma Metropolitana-Xochimilco, C. P. 04960, México, DF, Mexico

<sup>c</sup>Departamento de Química, Universidad Autónoma Metropolitana-Iztapalapa, Apdo. Postal 55-534, C. P. 09340, México, DF, Mexico

† Present address: Centro de Investigación y Desarrollo Tecnológico en Electroquímica, Parque Tecnológico Querétaro Sanfandila, 76703, Pedro Escobedo, Querétaro, México. Email: ultrabuho@yahoo.com.mx; Email: cfrontana@cideteq.mx; Fax: 52 442 211 60 01; Tel: 52 442 211 60 00, Ext: 7849.

quinone, rather than relying on redox potentials obtained in the course of a single low-concentration experiment.

Concerning the site where this type of compounds can act, it should be noted that certain organelles present in the cell or even at the cellular membrane act as non-aqueous media, where formation and stability of radical anions can be increased.<sup>24,25</sup> In this context, the studies performed under aprotic conditions are useful to study radical anion intermediates, which are quite difficult to be characterized in protic medium, such as water. Also, the aprotic environment of the cell membrane can be mimicked by the employed media. The employment of electrochemical methods in non-aqueous solutions allows a reduction of the reactivity of such radicals, facilitating the acquisition of data not only on thermodynamics properties but also on their kinetic aspects of formation and degradation.<sup>26–32</sup> Consequently, the use of these methods in non-aqueous media can provide a better alternative for studying and characterizing the stability of electrogenerated radicals which complements the results obtained during *in vivo* analysis.<sup>18–25</sup>

In this work, an electrochemical study of the reactivity of electrogenerated radicals for two naturally occurring quinones in DMSO (juglone **2** and plumbagin **4**, Fig. 1) is presented. The choice of the 5-hydroxy-1,4-naphthoquinones was made because there are an important number of research papers comparing their toxicity but not fully assessing the stability of the radicals that were generated.<sup>19–22,24,33–38</sup> A characterization based on the employment of cyclic voltammetry and ESR-spectroelectrochemical method was conducted for this work.<sup>30,32,39</sup>

## Experimental section

Juglone (**2**, Fig. 1) and plumbagin (**4**) were employed (Aldrich, R. A. Grade) without further purification. Dimethyl sulfoxide (DMSO, Uvasol, spectroscopic quality) was treated with 3 Å molecular sieves (Merck) before its use. Recrystallized tetrabutylammonium hexafluorophosphate (Fluka Chemika, Electrochemical grade, But<sub>4</sub>PF<sub>6</sub>), was used as the supporting electrolyte.

Cyclic voltammetry experiments were performed with an AUTOLAB PGSTAT 100 potentiostat/galvanostat. IR Drop correction was performed during all of the experiments, using  $R_u$  values obtained with the positive feedback technique until potentiostat instability was reached.<sup>40,41</sup> A conventional three electrode cell was used to carry out these experiments. A glassy carbon microelectrode (Surface: 0.07 cm<sup>2</sup>), was used as the working electrode. Prior to its use it was polished with 0.05 μm alumina (Bühler), sonicated in distilled water for 10 minutes and rinsed with acetone. The electrode was rinsed with acetone between each voltammetric run for each concentration. Electrode polishing procedure was performed when a change in solution concentration was required. A platinum mesh was used as an auxiliary electrode. Potential values were obtained *versus* a commercial saturated calomel electrode (SCE) separated from the solution by a salt bridge and referenced to the ferricinium/ferrocene couple (Fc<sup>+</sup>/Fc) according to the IUPAC recommendation.<sup>42</sup> Potential values were independently measured for each solution in order to avoid potential changes due to experimental manipulations. The potential of the redox couple *versus* the reference electrode was 0.40 ± 0.01 V. Electrochemical experiments were made employing solutions of juglone and plumbagin concentrations in

the range from 1 to 22 × 10<sup>-3</sup> mol L<sup>-1</sup> dissolved in 0.2 mol L<sup>-1</sup> But<sub>4</sub>PF<sub>6</sub>/DMSO. Tetrafluoroboric acid (Aldrich®) 48% solution in water was also employed for experiments under the presence of acid. Cyclic voltammetry experiments were performed with these prepared solutions.

ESR spectra were recorded in the X band (9.85 GHz), using a Bruker EMXplus instrument with a rectangular TE<sub>102</sub> cavity. A commercially available spectroelectrochemical cell (Wilmad) was used. A platinum mesh (≈ 0.2 cm<sup>2</sup>) working electrode was introduced in the flat path of the cell. Another platinum wire was used as an auxiliary electrode (2.5 cm<sup>2</sup>). The reference electrode Ag/0.01 mol L<sup>-1</sup> AgNO<sub>3</sub> + 0.1 mol L<sup>-1</sup> tetrabutylammonium perchlorate in acetonitrile (Bioanalytical Systems, BAS) was employed as the reference electrode. Potential sweep control was performed with an AUTOLAB/PGSTAT 100 potentiostat. Quinone solutions of different concentrations in the range of 0.07 to 10 × 10<sup>-3</sup> mol L<sup>-1</sup> concentration were used for spectroelectrochemical experiments. These solutions were prepared by dissolving the compound in 0.2 mol L<sup>-1</sup> But<sub>4</sub>PF<sub>6</sub> in DMSO. The prepared solutions were deoxygenated for 30 minutes prior to each experiment and the cell was kept under an argon atmosphere (grade 5, Praxair) throughout the experiment. PEST WinSim free software Version 0.96 (National Institute of Environmental Health Sciences) was used to perform ESR spectra simulations. Measured hyperfine coupling constant values (HFCC, *a*) were compared to the simulated values. This program was also useful to evaluate HFCC values in the case where a direct measurement would be difficult under the spectra acquisition conditions.

ZINDO/1 calculations<sup>43,44</sup> were performed with HyperChem (HyperCube Inc.) Ver. 7.51 to perform full geometry optimizations (no geometry constraints) for the radical structures experimentally detected by employing UHF (Unrestricted Hartree Fock) calculations for open-shell systems. This method has been useful in evaluating electronic properties for these types of quinones.<sup>45</sup> Vibrational analysis was performed to check that the obtained structures were indeed the minimum energy conformers, characterized by the lack of negative vibrational frequencies. These structures were used as inputs for single point calculations performed at the same theoretical level. From these data, spin densities were evaluated as the difference between  $\alpha$  and  $\beta$  spin densities for the corresponding H atoms as previously described.<sup>40</sup>

## Results and discussion

### Cyclic voltammetry of juglone and plumbagin in DMSO

Fig. 2 shows the cyclic voltammograms obtained for the quinones being studied. The resulting voltammograms show typical two successive one-electron reduction processes (for juglone peaks Ic and Iic, Fig. 2A, and for plumbagin peaks Ic' and Iic', Fig. 2B) which occurs for quinones in aprotic media.<sup>46,47</sup> The first electron transfer corresponds to the reduction of the quinone (represented as *Q*) into a radical anion or semiquinone (*Q*<sup>-</sup>, eqn 1), while the second is associated with the reduction of the semiquinone into a dianion species (*Q*<sup>2-</sup>, eqn 2).



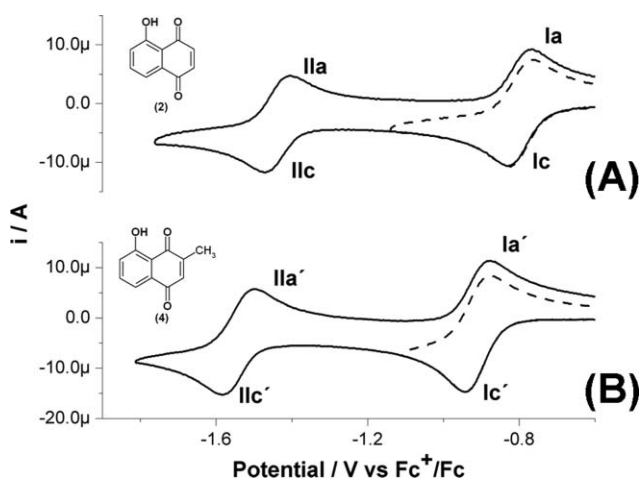


**Fig. 2** Cyclic voltammograms for  $1 \times 10^{-3}$  mol L $^{-1}$  solutions of (A) juglone **2** and (B) plumbagin **4** in 0.2 mol L $^{-1}$  But $_4$ PF $_6$ /DMSO. WE: GC (0.07 cm $^2$ );  $\nu = 100$  mVs $^{-1}$ . Two inversion potential conditions are shown for each compound.

Both electron uptakes are electrochemically reversible as shown by the anodic peaks that appeared (peaks Ia and IIa for **2**, Ia' and IIa' for **4**,  $\Delta E_{\text{plc-Ia}} = 55$  mV,  $\Delta E_{\text{plc-IIa}} = 62$  mV,  $\Delta E_{\text{plc-Ia'}} = 63$  mV,  $\Delta E_{\text{plc-IIa'}} = 65$  mV). However, the signals observed experimentally appear at different potential values for each studied quinone, as the peak Ic for juglone appears at a less negative potential than the corresponding peak for plumbagin ( $E_{\text{plc}}(\mathbf{2}) = -0.83$  V vs Fc $^+$ /Fc,  $E_{\text{plc}}(\mathbf{4}) = -0.94$  V vs Fc $^+$ /Fc). This difference is attributed to the electron-donating nature of the  $-\text{CH}_3$  group at position C-2 for plumbagin, which shifts the potential value for the correspondingly substituted quinone to a more negative potential value than the corresponding reduction process for juglone, which bears an  $-\text{H}$  substituent.<sup>48–50</sup>

As commented above, the reduction potential ( $E_{1/2}$  or  $E^0$ ), is used as a parameter for understanding the differences in reactivity of these quinones.<sup>24</sup> As it has been shown that differences in the cytotoxic effects can occur upon changes in the concentration of juglone and plumbagin,<sup>24</sup> it would be useful to evaluate the electrochemical behavior during experiments at different concentrations of each quinone, rather than relying on the study of a single concentration. To reveal the influence of the quinone concentration on the stability of the semiquinone and dianion intermediates, cyclic voltammograms for juglone and plumbagin at different concentrations were performed and are presented in Figs. 3 and 4.

From these voltammograms, a difference in the electrochemical behavior for both quinones can be observed. While for plumbagin only slight changes in the voltammetric curve are visible for peaks Ia/Ic (Fig. 3B), peak Ia for juglone shows a progressive diminishment in current values upon the increase of concentration (Fig. 3A). Since these voltammetric signals are associated to the formation of the semiquinone species (peak Ic) and to their corresponding re-oxidation (peak Ia), the observed differences indicate that the stability of the radical anion generated from juglone is determined by the amount of this species that is present at the electrode. This feature has consequences in the subsequent reduction process of the radical anion into a dianion species (Fig. 4A). For juglone, a progressive diminishment in current

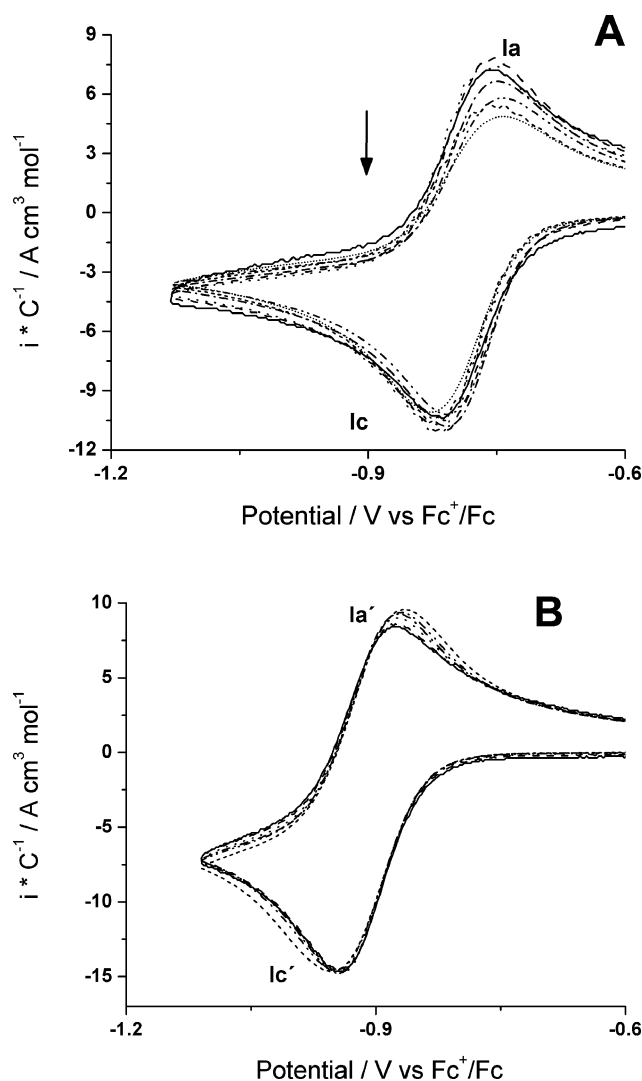


**Fig. 3** Cyclic voltammograms for solutions of increasing concentrations of (A) juglone **2** and (B) plumbagin **4** in 0.2 mol L $^{-1}$  But $_4$ PF $_6$ /DMSO. WE: GC (0.07 cm $^2$ );  $\nu = 100$  mVs $^{-1}$ .  $E_{\text{c}}$ : (A)  $-1.15$ ; (B)  $-1.10$  V vs Fc $^+$ /Fc. Increasing concentration values: (—) 1; (---) 3.1; ( $\cdots$ ) 5.2; (---) 10; (---) 14 and (---) 18  $\times 10^{-3}$  mol L $^{-1}$ . Arrows indicate the changes occurring under progressive increases in concentration of each quinone.

also appeared for higher concentrations of the quinone, while no changes in voltammetric behavior occurred for the semiquinone generated from plumbagin at higher concentrations of the quinone (Fig. 4B). These findings indicate that in the case of juglone, the process consumed the electrogenerated radical anion after its generation. In view of the small structural difference between juglone and plumbagin (Fig. 1) and the large difference in their electrochemical behavior, it is necessary to understand the chemical nature of the radicals being generated at signals Ic. Thus spectroelectrochemical-electron spin resonance analysis was employed.

#### Spectroelectrochemical-ESR study of the electrogenerated radical anions for juglone and plumbagin

ESR spectra of the electrogenerated radical anions for juglone and plumbagin for  $1 \times 10^{-3}$  mol L $^{-1}$  concentrations were conducted by

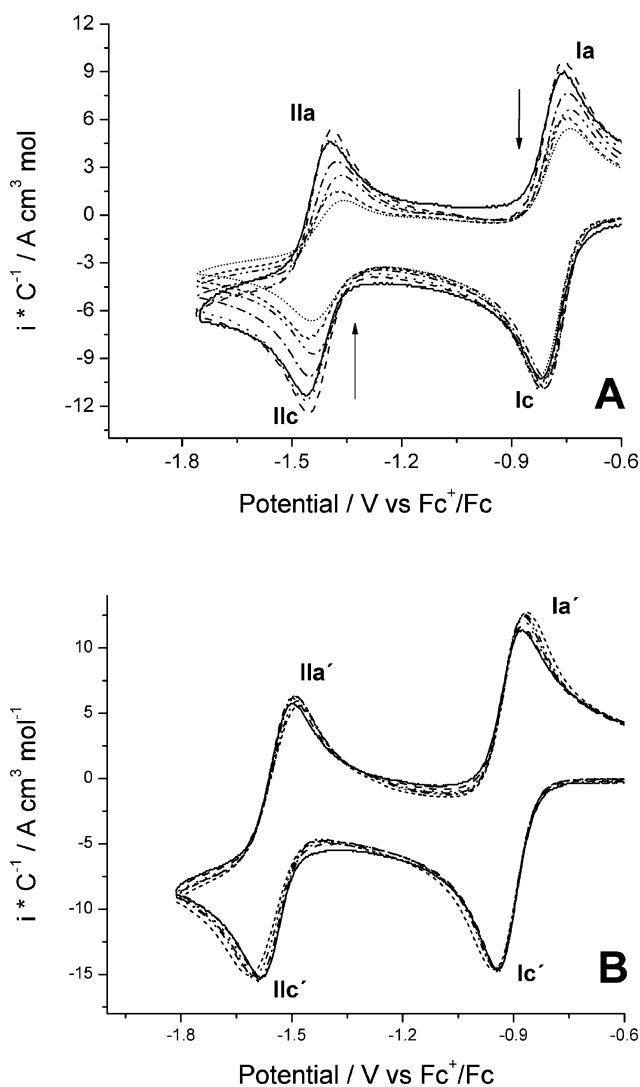


**Fig. 4** Cyclic voltammograms for solutions of increasing concentrations of (A) juglone **2** and (B) plumbagin **4** in 0.2 mol L<sup>-1</sup> But<sub>4</sub>PF<sub>6</sub>/DMSO. WE: GC (0.07 cm<sup>2</sup>);  $\nu = 100$  mVs<sup>-1</sup>.  $E_{\lambda}$ : (A) -1.75; (B) -1.80 V vs Fc<sup>+</sup>/Fc. Increasing concentration values: (—) 1; (---) 3.1; (···) 5.2; (---) 10; (---) 14 and (---) 18 × 10<sup>-3</sup> mol L<sup>-1</sup>. Arrows indicate the changes occurring under progressive increases in concentration of each quinone.

applying potential values after peaks Ic and Ic' (Fig. 2) as shown in Fig. 5.

The radical species detected are the corresponding semiquinones of juglone (Fig. 5A) and plumbagin (Fig. 5B). In the case of juglone, the observed spectrum is characterized by the presence of 6 HFCC values, each corresponding to the Hydrogen atom that interacted with the unpaired electronic spin (Table 1).

**Table 1** HFCC values and  $g$  factors of the semiquinone structures of the studied quinones <sup>a, b</sup>

Compound	H <sub>2</sub> /Gauss	H <sub>3</sub> /Gauss	H <sub>5</sub> /Gauss	H <sub>6</sub> /Gauss	H <sub>7</sub> /Gauss	H <sub>8</sub> /Gauss	$g$
Juglone <b>2</b>	4.05	2.53	0.36 (-OH)	0.75	1.02	0.82	2.0074
Plumbagin <b>4</b>	2.7 (-CH <sub>3</sub> )	1.90	0.27 (-OH)	1.20	0.77	3.20	2.0084

<sup>a</sup> Assignments for each hyperfine coupling constant with the corresponding hydrogen atom are indicated for each signal (See Fig. 1 for numbering).

<sup>b</sup> Radicals obtained upon reduction at  $E_{\text{appl}} = -1.1$  V vs Fc<sup>+</sup>/Fc.

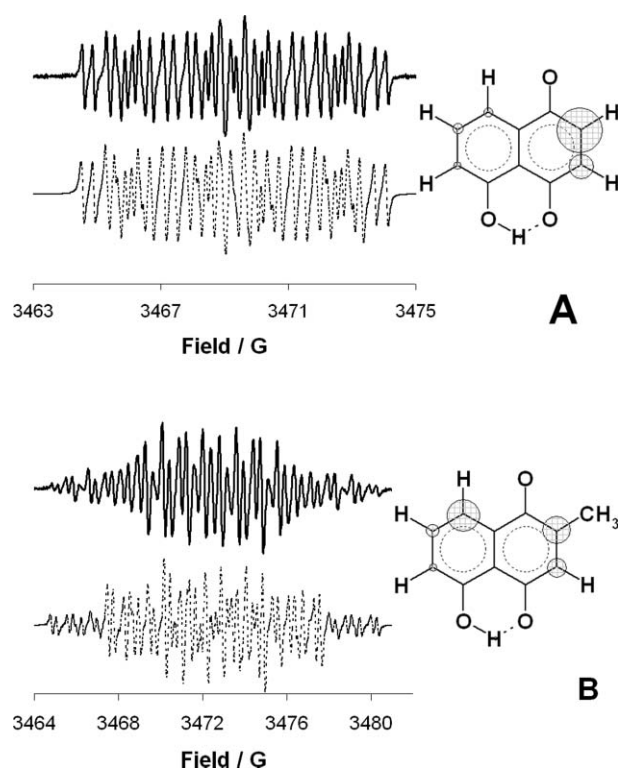


**Fig. 5** ESR spectra for the electrogenerated radical anions from 1 × 10<sup>-3</sup> mol L<sup>-1</sup> solutions of (A) juglone **2** and (B) plumbagin **4** in 0.2 mol L<sup>-1</sup> But<sub>4</sub>PF<sub>6</sub>/DMSO. WE: Pt (0.7 cm<sup>2</sup>). Spin density structures as evaluated from calculations and experimental data are sketched at each spectrum. Solid upper line: experimental data; dashed lower line: isotropic simulation.

In the case of plumbagin, 6 HFCC values also appear, but one of them is related to the interaction with the H atoms at the CH<sub>3</sub> residue at position C-2 (Fig. 1), accounting for a triplet structure, while the remaining H atoms show their corresponding HFCC values (Table 1). Assignment of each HFCC value was performed by electronic structure calculations of the spin density and related to data obtained with the experimental HFCC values, denoted as  $a$ , through the use of the McConnell equation (Fig. 5).<sup>50-52</sup>

$$a = Qp \quad (3)$$

Upon increasing the quinone concentration, spectra for the electrogenerated radical anion of juglone **2** evolved into another structure (Fig. 6A) while no change in the hyperfine structure was evident for plumbagin (Fig. 6B). In agreement with the results obtained during the voltammetric study, this result shows that for juglone, the electrogenerated radical anion evolves into another radical species during the course of a chemical process. Both species seem to coexist at intermediate concentrations

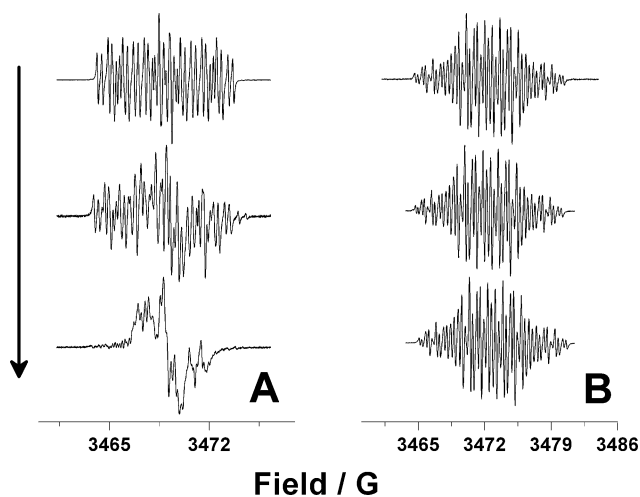


**Fig. 6** Evolution of ESR spectra for solutions of (A) juglone **2** and (B) plumbagin **4** in  $0.2 \text{ mol L}^{-1}$   $\text{But}_4\text{PF}_6/\text{DMSO}$ . WE: Pt ( $0.7 \text{ cm}^2$ ). Data represented spectrum from top to bottom are 1, 3 and  $10 \times 10^{-3} \text{ mol L}^{-1}$  solutions of each quinone. Arrow indicates direction of increasing concentration of each quinone.

( $1-10 \times 10^{-3} \text{ mol L}^{-1}$ , Fig. 6A). ESR spectra obtained at high concentration for juglone did not allow for the evaluation of the chemical nature of the radical generated due to mixing of HFCC data (Fig. 6A). Chemical evolution of the radical was tested by evaluating the number of spins in solution by double integration of the spectra and by comparing the data obtained for each concentration (Fig. 7).

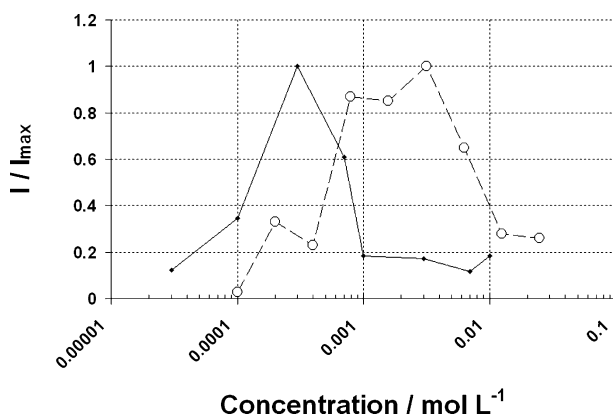


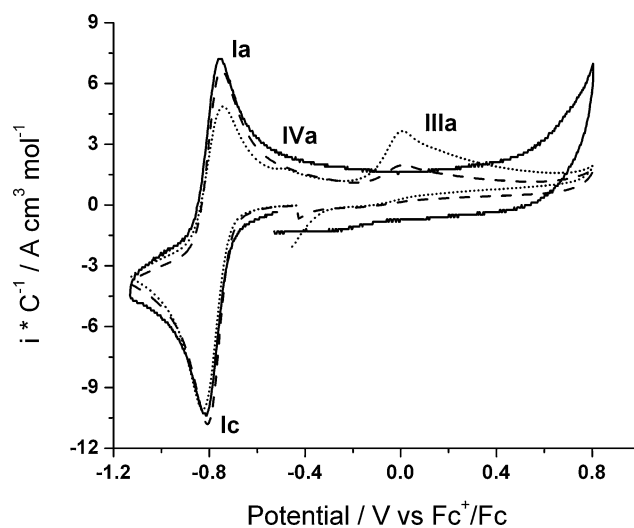
**Fig. 7** Normalized integral intensity ( $I$ ) for ESR spectra of (◆) juglone **2** and (○) plumbagin **4** as a function of the concentration of each quinone.

Integrated data obtained show that formation of the radical anion for juglone reaches its maximum in terms of total signal at concentrations in the range of  $3 \times 10^{-4} \text{ mol L}^{-1}$  (Fig. 7). After this value, the number of radicals generated diminishes sharply and does not increase proportionally to the concentration of the quinone in solution. For plumbagin, this effect occurs at concentrations near  $5 \times 10^{-3} \text{ mol L}^{-1}$  (Fig. 7). However, in this case, the observed radical anion does not evolve chemically as occurred for juglone (Fig. 6), which indicates that the observed decrease in concentration could be associated to homogeneous broadening of the ESR signal through mechanisms involving

spin–spin interactions due to the high concentrations of the electrochemically generated radicals.<sup>53</sup>

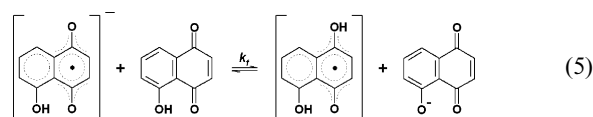
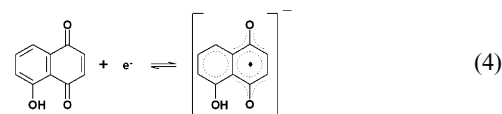
#### Analysis of the reduction mechanism for juglone at high concentrations

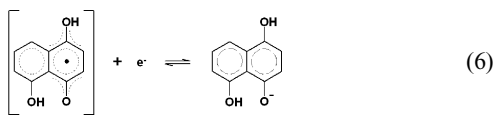
With the results presented above, the chemical pathway involved in the evolution of the radical anion of juglone needs to be defined. For this purpose, a more detailed voltammetric analysis was performed. Upon extension of the inversion potential for the return voltammetric scan (Fig. 8), a new anodic signal appears, named IIIa, at a peak potential  $E_p$  value of  $10 \text{ mV vs Fc}^+/\text{Fc}$ . Upon higher concentrations of juglone, another oxidation signal begins to appear, named IVa, at a less positive peak potential value than for signal IIIa ( $E_{p\text{IVa}} = -0.48 \text{ V vs Fc}^+/\text{Fc}$ ). Both oxidation signals are associated to the consumption of the semiquinone species, as they appear upon inverting the potential scan just after peak Ic (see Section 1). Signal IVa presented a significantly higher intensity at higher concentrations of the quinone. This behavior is consistent with the existence of coupled chemical processes after an electron uptake reaction.<sup>31,32,54,55</sup>



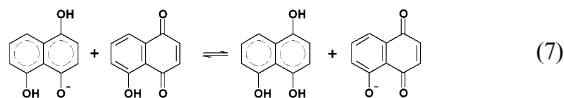
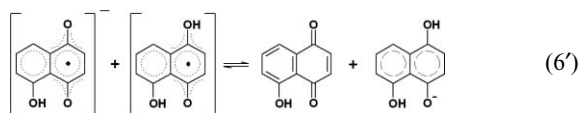
**Fig. 8** Cyclic voltammograms for solutions of increasing concentrations of juglone **2** in  $0.2 \text{ mol L}^{-1}$   $\text{But}_4\text{PF}_6/\text{DMSO}$ . WE: GC ( $0.07 \text{ cm}^2$ );  $\nu = 100 \text{ mVs}^{-1}$ .  $E_\lambda$ : (A)  $-1.75$ ; (B)  $-1.80 \text{ V vs Fc}^+/\text{Fc}$ . Increasing concentration values: (—) 1; (---)  $5.2$  and ( $\cdots$ )  $18 \times 10^{-3} \text{ mol L}^{-1}$ .

Based on the results previously presented for other types of hydroxyquinones, signals IIIa and IVa are related to the oxidation of the hydroquinone forms of juglone.<sup>31</sup> Accordingly, the proton at position C-5 in juglone **2** (Fig. 1) bears mild acidic characteristics, and thus the mechanism that occurs at peak Ic can be described as follows:





or



This process is different compared with the typical two-electron reduction occurring at low concentration values of juglone, as described above (eqn 1 and 2). For instance, the semiquinone intermediate formed during the first electron transfer (eqn 4) takes a proton from unreduced juglone present in solution, thus generating a protonated semiquinone (eqn 5). This product can be reduced at the applied potential condition at peak Ic or by the more reactive semiquinone, thus generating an hydroquinone semiprotonated species (eqn 6 or eqn 6').<sup>31,32</sup> In forthcoming steps, this species can uptake another proton to generate protonated hydroquinone (eqn 7), although this process would require an even higher amount of juglone as it is the only source of protons in solution. Thus, the peak IIIa could be associated with the oxidation of the semiprotonated hydroquinone form generated during eqn 6 or 6', while the small peak IVa is related to the oxidation of the excess of protonated semiquinone since the amount of this intermediate becomes higher with the increasing concentrations of juglone. In order to test this proposal, a voltammetric study on juglone **2** in the presence of a strong proton donor was performed, so the mechanism can be directed towards the formation of the hydroquinone (Fig. 9).<sup>31</sup>

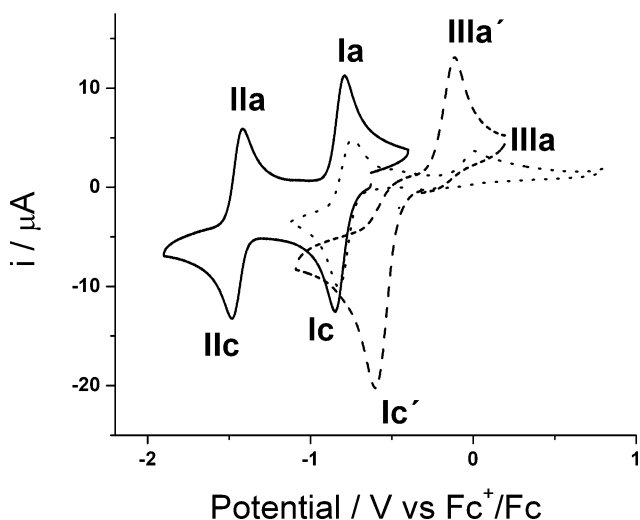


**Fig. 9** Cyclic voltammograms for (—)  $1 \times 10^{-3} \text{ mol L}^{-1}$  and (···)  $18 \times 10^{-3} \text{ mol L}^{-1}$  solutions of juglone **2** in  $0.2 \text{ mol L}^{-1} \text{ But}_4\text{PF}_6/\text{DMSO}$ . (---)  $1 \times 10^{-3} \text{ mol L}^{-1}$  solution of  $20 \times 10^{-3} \text{ mol L}^{-1}$  juglone **2** in the presence of  $20 \times 10^{-3} \text{ mol L}^{-1}$  tetrafluoroboric acid. WE: GC ( $0.07 \text{ cm}^2$ );  $v = 100 \text{ mVs}^{-1}$ .

In Fig. 9, the solid line corresponds to the voltammetric behaviour of  $1 \times 10^{-3} \text{ mol L}^{-1}$  juglone **2**, while the dotted line

represents the voltammetric trace of the same quinone at  $18 \times 10^{-3} \text{ mol L}^{-1}$ . Dashed line corresponds to the behaviour of a  $1 \times 10^{-3} \text{ mol L}^{-1}$  solution of juglone **2** mM in the presence of  $20 \text{ mM}$  tetrafluoroboric acid. In this last trace, the first electron transfer becomes a two electron process, forming the hydroquinone form, which is oxidized at peak IIIa'. This peak occurs about  $100 \text{ mV}$  less positive than the corresponding peak IIIa for the experiment performed at an excess amount of the quinone. This difference in behaviour can be related to the capacity of the hydroquinone of being associated in solution with the corresponding anions from either the electrolyte or the deprotonated form of the quinone.<sup>31</sup> This association process can change the position of the corresponding oxidation peak by the amount indicated. This result allows to confirm the presence of the hydroquinone during the reverse scan presented for solutions with excess concentrations of juglone (Fig. 8). The nature of peak IVa could also be related to the oxidation of the deprotonated form of the hydroquinone, as occurs during the analog oxidation processes of phenols and phenolate anions into the corresponding cation radical species.<sup>56-59</sup>

This proposal considers both the behavior at low and high concentrations of the quinone. For example, at low concentrations of juglone, the reduction process at peak Ic behaves as a monoelectronic electron transfer process (eqn 4), thus avoiding protonation step (eqn 5) and leading to a consecutive electron transfer process (as presented in eqn 1 and 2). The proposed mechanism at the reduction peak Ic, at high concentrations, involves a proton transfer reaction (eqn 5) leading to the formation of a second radical species. The presence of this protonated radical has already been described and has been detected by pulse radiolysis studies.<sup>60</sup> It is stable enough to be detected in the spectroelectrochemical-ESR measurements, thus explaining the mixture of radical species ( $Q^{\cdot-}$  and  $HQ^{\cdot}$ ) observed for juglone at high concentrations (Fig. 6). However, this protonation reaction would be quite slow since the electrochemical reversibility is kept at the process Ia/Ic in the voltammetric behavior. It is therefore possible to estimate the kinetic constant for this second order reaction ( $k_f$ , eqn 5) by modeling the measured peak current ratio between signals Ia/Ic, setting up the above proposed model in a voltammetric simulation program (DigiElch 4.5®).<sup>61-66</sup> In this way, a series of theoretical working curves were constructed by inputting several values of  $k_f$ , and comparing the experimental ratio at different concentrations of juglone (Fig. 10).

The experimental  $k_f$  was found to be in the range of  $1.8\text{--}2.1 \text{ M}^{-1}$ , considering the second order reaction mechanism involved (eqn 4-7). This value indicates a low rate for protonation processes in aprotic solvents.<sup>40,55</sup> It should be noted that the existence of this chemical pathway has not been considered earlier during studies with juglone although it is prevalent during the reduction of  $\alpha$ -hydroxyquinones.<sup>32,54</sup> The rate of this protonation has proven to be controlled due to inductive effects provoked by substituents in the structure,<sup>40</sup> as is the case for plumbagin. In this compound, the  $\text{CH}_3$  residue at position C-2 acts as an electron-donating substituent,<sup>48-50</sup> not only promoting the mentioned shift in potential values with respect to juglone, but also diminishing the rate of protonation to an extent where, at the concentration values used in this work, no evidence of its occurrence was found.

The existence of this sequence could provide an alternative mechanisms for understanding differences in behavior when comparing biological activities of juglone and plumbagin. As

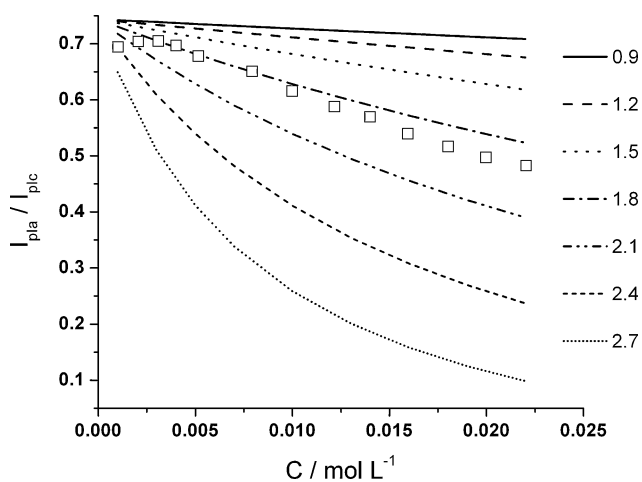


**Fig. 10** Working curves for the ratio  $I_{\text{pla}}/I_{\text{plc}}$  for juglone **2** as a function of the concentration of the quinone, for different values of  $k_f$ . Theoretical calculated curves are shown as lines; squares represent experimental data.

commented above, upon comparing cytotoxic activity of both quinones, a difference has been found. This difference has been related to their redox cycling capacity, as plumbagin maintains its activity towards hydrogen peroxide production and oxidation of glutathione.<sup>36</sup> In the same study, during quinone reductase induction studies juglone more than plumbagin increased the specific activity of the enzyme.<sup>36</sup> This has been tested in gastrointestinal tissues where differences occur presumably due to different pH gradients at each section.<sup>67,68</sup> This activity could be explained by the ease by which juglone forms hydroquinone species as shown in this study. Considering the increasing amount of specialized literature related to these compounds, the present study could provide a strategy for evaluating the reasons for activity differences at the molecular level.

## Conclusions

An electrochemical and spectroelectrochemical study is presented for evaluating reactivity differences in the semiquinone anions from naturally occurring quinones juglone (5-hydroxy-1,4-naphthoquinone) and plumbagin (2-methyl-8-hydroxy-1,4-naphthoquinone) is presented. By employing cyclic voltammetry and *in situ* spectroelectrochemical Electron Spin Resonance measurements, it was found that while semiquinone species generated from plumbagin are stable radical anions in DMSO solution, the species generated from juglone are more reactive at concentrations of nearly  $3 \times 10^{-3} \text{ mol L}^{-1}$  based on the lack of reversibility in the corresponding voltammetric signals. Semiquinones from juglone are involved in a self-protonation process at a slow rate of protonation ( $1.8\text{--}2.1 \text{ M}^{-1}$ ), due to the mild acidity of the OH group at the C-5 position. This result is important when considering observed differences in biochemical reactivity for these quinones, particularly in cases where mediated cytotoxic action is provoked by these agents.

## Acknowledgements

C. Frontana thanks CONACyT-Mexico for postdoctoral support through the programs “Apoyos para la Formación de Doctores

en Ciencias” and “Estancias Postdoctorales y Sabáticas 2007”. L. Hernández-Muñoz thanks CONACyT-Mexico for financial support for her Ph. D. studies.

## References

- G. L. McNew, *Bull. Torrey Bot. Club.*, 1950, **77**, 294–297.
- T. J. Monks and D. C. Jones, *Curr. Drug. Metab.*, 2002, **3**, 425–438.
- Z. F. Plyta, T. Li, V. P. Papageorgiou, A. S. Mellidis, A. S. A. N. Assimopoulou, E. N. Pitsinos and E. A. Couladouros, *Bioorg. Med. Chem. Lett.*, 1998, **8**, 3385–3390.
- V. P. Papageorgiou, A. N. Assimopoulou, E. A. Couladouros, D. Hepworth and K. C. Nicolaou, *Angew. Chem., Int. Ed.*, 1999, **38**, 271–300.
- J. Grolig and R. Wagner, Naphthoquinones, in: *Ullmann's Encyclopedia of Industrial Chemistry*, Germany, Wiley-VCH Verlag GmbH & Co, 2005, vol. 22, pp. 471, 10.1002/14356007.a17\_067.
- M. Shi, E. Gozal, H. A. Choy and H. J. Forman, *Free Radic. Biol. Med.*, 1993, **15**, 57–67.
- H. S. Schwartz and P. M. Kanter, *Cancer Treatment Reports*, 1979, **63**, 821–825.
- F. Arcamone, *Cancer Research*, 1985, **45**, 5995–5999.
- P. F. Conte, *Bull. Cancer*, 1993, **80**, 152–155.
- R. S. Teixeira, C. J. Valduga, L. A. Benvenuti, S. Schreier and R. C. Maranhao, *J. Pharm. Pharmacol.*, 2008, **60**, 1287–1295.
- P. Tardi, S. Johnstone, N. Harasym, S. Xie, T. Harasym, N. Zisman, P. Harvie, D. Bermudes and L. Mayer, *Leukemia Res.*, 2009, **33**, 129–139.
- E. M. Perchellet, M. J. Magill, X. Huang, D. M. Dalke, D. H. Hua and J. P. Perchellet, *Anti-Cancer Drugs*, 2000, **11**, 339–352.
- T. Fukushima, Y. Kawai, T. Nakayama, T. Yamauchi, A. Yoshida, Y. Urasaki, S. Imamura, K.-I. Kamiya, H. Tsutani, T. Ueda and T. Nakamura, *Oncol. Res.*, 1996, **8**, 95–100.
- S. H. Kim and H. J. Lee, *Repub. Korean Kongkae Taeho Kongbo* 2006, CODEN: KRXXA7 KR 2006007967 A 20060126 CAN 145:403976 AN 2006:1034723.
- Y. Chung, Y.-K. Shin, C.-G. Zhan, S. Lee and H. Cho, *Arch. Pharmac. Res.*, 2004, **27**, 893–900.
- O. Moullet and J. L. Dreyer, *Biochem. J.*, 1994, **300**, 99–106.
- N. Gokhale, S. Padhye, C. Newton and R. Pritchard, *Metal-Based Drugs*, 2000, **7**, 121–128.
- A. Chichirau, M. Fluerau, L. L. Chepelev, J. S. Wright, W. G. Willmore, T. Durst, H. H. Hussain and M. Charron, *Free Radic. Biol. Med.*, 2005, **38**, 344–355.
- H. Babich and A. Stern, *J. Appl. Toxicol.*, 1993, **13**, 353–358.
- K. Ollinger and A. Brunmark, *J. Biol. Chem.*, 1991, **266**, 21496–21503.
- M. Y. Lim, J. H. Jeon, E. Y. Jeong, C. H. Lee and H. S. Lee, *Food Chem.*, 2006, **100**, 1254–1258.
- T. W. Schultz and A. P. Bearden, *Bull. Environ. Contam. Toxicol.*, 1998, **61**, 405–410.
- P. J. O'Brien, *Chem.-Biol. Interact.*, 1991, **80**, 1–41.
- J. J. Inbaraj and C. F. Chignell, *Chem. Res. Toxicol.*, 2004, **17**, 55–62.
- G. Tudor, P. Gutierrez, A. Aguilera-Gutierrez and E. A. Sausville, *Biochem. Pharmacol.*, 2003, **65**, 1061–1075.
- M. Aguilar-Martínez, J. A. Bautista-Martínez, N. Macías-Ruvalcaba, I. González, E. Tovar, T. Marin, del Alizal, O. Collera and G. Cuevas, *J. Org. Chem.*, 2001, **66**, 8349–8363.
- M. Gómez, F. J. González and I. González, *J. Electrochem. Soc.*, 2003, **150**, E527–E534.
- M. Aguilar-Martínez, N. A. Macías-Ruvalcaba, J. A. Bautista-Martínez, M. Gómez, F. J. González and I. González, *Curr. Org. Chem.*, 2004, **8**, 1721–1738.
- M. Gómez, F. J. González and I. González, *J. Electroanal. Chem.*, 2005, **578**, 193–202.
- C. Frontana and I. González, *J. Braz. Chem. Soc.*, 2005, **16**, 299–307.
- P. D. Astudillo, J. Tiburcio and F. J. Gonzalez, *J. Electroanal. Chem.*, 2007, **604**, 57–64.
- C. Frontana and I. González, *J. Electroanal. Chem.*, 2007, **603**, 155–165.
- C. F. Chignell and R. H. Sik, *Free Radic. Biol. Med.*, 2003, **34**, 1029–1034.
- E. de Castro, S. H. de Castro and T. E. Johnson, *Free Radic. Biol. Med.*, 2004, **37**, 139–145.
- R. V. Satyanarayana Rao and G. T. Gujar, *Entomol. Exp. Appl.*, 1995, **77**, 189–192.

- 36 R. Munday and C. M. Munday, *Planta Medica.*, 2000, **66**, 399–402.
- 37 L. Miseviciene, Z. Anusevicius, J. Sarlauskas, R. J. Harris, N. S. Scrutton and N. Cenas, *Acta Biochim. Pol.*, 2007, **54**, 379–385.
- 38 D. A. Wright, R. Dawson, S. J. Cutler, H. G. Cutler, C. E. Orano-Dawson and E. Graneli, *Water Res.*, 2007, **41**, 1294–1302.
- 39 D. M. Hernandez, M. A. B. F. de Moura, D. P. Valencia, F. J. Gonzalez, I. Gonzalez, F. C. de Abreu, E. N. da Silva Junior, V. F. Ferreira, A. Ventura, Pinto, M. O. F. Goulart and C. Frontana, *Org. Biomol. Chem.*, 2008, **6**, 3414–3420.
- 40 J. A. Morales-Morales, C. Frontana, M. Aguilar-Martínez, J. A. Bautista-Martínez, F. J. Gonzalez and I. Gonzalez, *J. Phys. Chem. A.*, 2007, **111**, 8993–9002.
- 41 J. M. Savéant, *Elements of Molecular and Biomolecular Electrochemistry: An Electrochemical Approach to Electron Transfer Chemistry*, New Jersey, Wiley Interscience, 2006.
- 42 G. Gritzner and J. Kůta, *Pure Appl. Chem.*, 1984, **4**, 461–466.
- 43 J. D. Head and M. C. Zerner, *Chem. Phys. Lett.*, 1985, **122**, 264–270.
- 44 J. D. Head and M. C. Zerner, *Chem. Phys. Lett.*, 1986, **131**, 359–366.
- 45 M. S. Khan and Z. H. Khan, *Spectrochim. Acta A*, 2005, **61**, 777–790.
- 46 A. Capon and R. J. Parsons, *J. Electroanal. Chem.*, 1973, **46**, 215–222.
- 47 J. Q. Chambers, Electrochemistry of quinones, in *The Chemistry of Quinonoid Compounds, part 2*, ed. S. Patai, John Wiley & Sons, London, 1974, pp. 737–791.
- 48 L. P. Hammett, *J. Am. Chem. Soc.*, 1937, **59**, 96–103.
- 49 C. Hansch, A. Leo and R. W. Taft, *Chem. Rev.*, 1991, **91**, 165–195.
- 50 P. Zuman, *Substituent, Effects in Organic Polarography*, Plenum Press, New York, 1967.
- 51 H. M. McConnell, *J. Chem. Phys.*, 1956, **24**, 764–766.
- 52 H. M. McConnell and D. B. Chesnut, *J. Chem. Phys.*, 1958, **28**, 107–117.
- 53 J. A. Weil, J. R. Bolton, *Electron Paramagnetic Resonance: Elementary Theory and Practical Applications*, Wiley-Interscience, New Jersey, 2007.
- 54 F. J. González, J. M. Aceves, R. Miranda and I. González, *J. Electroanal. Chem.*, 1991, **310**, 293–303.
- 55 C. Amatore, G. Capobianco, G. Farnia, G. Sandoná, J. M. Saveant, M. G. Severin and E. Vianello, *J. Am. Chem. Soc.*, 1985, **107**, 1815–1824.
- 56 B. Speiser and A. Rieker, *J. Chem. Res.*, 1977, 314–315.
- 57 B. Speiser and A. Rieker, *J. Electroanal. Chem.*, 1979, **102**, 373–395.
- 58 B. Speiser and A. Rieker, *J. Electroanal. Chem.*, 1980, **110**, 231–246.
- 59 J. A. Richards and D. H. Evans, *J. Electroanal. Chem.*, 1977, **81**, 171–187.
- 60 J. Mukherjee, *Radiat. Phys. Chem.*, 1987, **29**, 455–462.
- 61 M. Rudolph, *J. Electroanal. Chem.*, 2003, **543**, 23–39.
- 62 M. Rudolph, *J. Electroanal. Chem.*, 2004, **571**, 289–307.
- 63 M. Rudolph, *J. Electroanal. Chem.*, 2003, **558**, 171–176.
- 64 M. Rudolph, *J. Comp. Chem.*, 2005, **26**, 619–632.
- 65 M. Rudolph, *J. Comp. Chem.*, 2005, **26**, 633–641.
- 66 M. Rudolph, *J. Comp. Chem.*, 2005, **26**, 1193–1204.
- 67 D. F. Evans, G. Pye, R. Bramley, A. G. Clark, T. J. Dyson and J. D. Hardcastle, *Gut.*, 1988, **29**, 1035–1041.
- 68 J. Fallingborg, L. A. Christensen, M. Ingeman-Nielsen, B. A. Jacobsen, K. Abildgaard, H. H. Rasmussen and S. N. Rasmussen, *J. Pediatr. Gastroenterol. Nutr.*, 1990, **11**, 211–214.